The antagonism of prostaglandin FP receptors inhibits the evolution of spreading depolarization in an experimental model of global forebrain ischemia

Dániel P. Varga[a,1], Írisz Szabó[a,1], Viktória É. Varga[a], Ákos Menhyárt[a], Orsolya M. Tóth[a], Mihály Kozma[b], Armand R. Bálint[a], István A. Krizbai[b,c], Ferenc Bari[a], Eszter Farkas[a,*]

[a] Department of Medical Physics and Informatics, Faculty of Medicine, University of Szeged; H-6720 Szeged, Korányi fasor 9, Hungary
[b] Physiology and Pathology of the Blood-Brain Barrier Research Group, Molecular Neurobiology Research Unit, Institute of Biophysics, Biological Research Centre, H-6726 Szeged, Temesvári krt. 62, Hungary
[c] Institute of Life Sciences, Vasile Goldis Western University; Revolutiei Blvd n°94, Arad 310025, Romania

ABSTRACT

Spontaneous, recurrent spreading depolarizations (SD) are increasingly more appreciated as a pathomechanism behind ischemic brain injuries. Although the prostaglandin F2α - FP receptor signaling pathway has been proposed to contribute to neurodegeneration, it has remained unexplored whether FP receptors are implicated in SD or the coupled cerebral blood flow (CBF) response. We set out here to test the hypothesis that FP receptor blockade may achieve neuroprotection by the inhibition of SD. Global forebrain ischemia/reperfusion was induced in anesthetized rats by the bilateral occlusion and later release of the common carotid arteries. An FP receptor antagonist (AL-8810; 1 mg/bwkg) or its vehicle were administered via the femoral vein 10 min later. Two open craniotomies on the right parietal bone served the elicitation of SD with 1 M KCl, and the acquisition of local field potential. CBF was monitored with laser speckle contrast imaging over the thinned parietal bone. Apoptosis and microglia activation, as well as FP receptor localization were evaluated with immunohistochemistry. The data demonstrate that the antagonism of FP receptors suppressed SD in the ischemic rat cerebral cortex and reduced the duration of recurrent SDs by facilitating repolarization. In parallel, FP receptor antagonism improved perfusion in the ischemic cerebral cortex, and attenuated hypoemic CBF responses associated with SD. Further, FP receptor antagonism appeared to restrain apoptotic cell death related to SD recurrence. In summary, the antagonism of FP receptors (located at the neuro-vascular unit, neurons, astrocytes and microglia) emerges as a promising approach to inhibit the evolution of SDs in cerebral ischemia.

1. Introduction

Spreading depolarization (SD), a remarkable neurophysiological phenomenon, has been recognized to be central to neurodegeneration after acute brain injury (Hartings et al., 2017a). Notably, recurrent SDs have been associated with early focal brain injury and delayed ischemic neurological deficit after subarachnoid hemorrhage (Dreier et al., 2006; Hartings et al., 2017b; Eriksen et al., 2019), and may provoke unfavorable hemodynamic and metabolic conditions in the cerebral cortex of malignant hemispheric stroke patients (Woitzik et al., 2013; Pinczolits et al., 2017).

SD corresponds to an abrupt, near complete breakdown of the

transmembrane ion gradients and a near-complete sustained neuronal and glial depolarization that propagates in the cerebral gray matter at a slow rate (2–8 mm/min) (Leão, 1944; Somjen, 2001). The restoration of the membrane potential requires the mobilization of metabolic resources for the operation of ATP-dependent ion pumps (e.g. the Na^+/K^+ ATP-ase). This need is met by a profound hyperemic cerebral blood flow (CBF) response coupled to SD in otherwise non-compromised tissue (Ayata and Lauritzen, 2015). The coupling between SD and local CBF becomes impaired under ischemia, which may create a metabolic supply-demand mismatch, a subsequent energy crisis superimposed on prevailing ischemia, and facilitated tissue injury (Dreier, 2011).

The current understanding of the relevance of SD in acute brain injuries posits that SD is harmful because its recurrence imposes an overwhelming metabolic challenge and triggers excitotoxicity in ischemic brain tissue (Hartings et al., 2017a; Shuttleworth et al., 2019). Consequently, the suppression of SD, or the improvement of the hemodynamic response to SD have been considered as therapeutic approaches in the post-operative care of brain injury patients (Helbok et al., 2019). Appreciating the cellular mechanisms of neurodegeneration triggered by SD (Hertelendy et al., 2019), the pharmacological modulation of SD has targeted (i) NMDA receptor-based glutamate excitotoxicity with the non-selective NMDA receptor blocker ketamine (Sánchez-Porras et al., 2017; Reinhart and Shuttleworth, 2018; Carlson et al., 2018), (ii) neurotoxic or vasoconstrictive intracellular Ca^{2+} accumulation by the L-type voltage-gated Ca^{2+} channel blocker nimodipine (Dreier et al., 2002; Carlson et al., 2019; Szabó, 2019), or (iii) SD-coupled spreading ischemia by the anti-coagulant and vasodilator agent cilostazol (Sugimoto et al., 2018).

We have gathered experimental evidence that prostaglandin signaling may be an additional target for neuroprotection in the context of SD (Varga et al., 2016). We have shown previously, that the antagonism of the EP4 receptor of prostaglandin E2 (PGE2) worsened the characteristics of SD (Varga et al., 2016). SD induces the release of arachidonic acid in the nervous tissue (Lauritzen et al., 1990) and the cyclooxygenase-based synthesis of a wide range of vasoactive arachidonic acid metabolites (Shibata et al., 1992). As such, the concentration of both the vasodilator PGE2 and the vasoconstrictor prostaglandin-F2α (PGF2α) was found to increase twofold in the cerebrospinal fluid in response to experimentally induced SD in rabbits. Treatment with the non-selective cyclooxygenase inhibitor indomethacin augmented the SD-coupled hyperemia, indicative of the dominant involvement of vasoconstrictive prostaglandins in the mediation of the CBF response (Shibata et al., 1992). Later, the more selective pharmacological inhibition of the EP4 receptor of PGE2 reduced the magnitude of hyperemia and augmented post-SD oligemia (Varga et al., 2016), while the antagonism of the FP receptor of PGF2α decreased the amplitude of post-SD oligemia in the otherwise intact rat cerebral cortex (Gariepy et al., 2017). These experimental data together suggest a fine balance of EP4 and FP receptor activation in the regulation of the CBF response to SD, and importantly, the vasoconstrictive contribution of the PGF2α – FP receptor signaling.

The PGF2α – FP receptor signaling cascade has been implicated in ischemia/reperfusion-induced neurodegeneration, as well. First, the level of PGF2α was shown to increase in the brain tissue and the cerebrospinal fluid in animal models of cerebral ischemia (Gaudet and Levine, 1980; Katz et al., 1988). Later, neurological deficit and ischemic lesion volume were found reduced in FP receptor knock-out compared to wild type mice (Saleem et al., 2009), and the pharmacological antagonism of FP receptors also resulted in smaller infarct volume and better functional outcome in a mouse model of focal cerebral ischemia (Kim et al., 2012). Further, the antagonism of FP receptors in an experimental model of traumatic brain injury – a disorder in which SD has been implicated (Hartings et al., 2011a,b; Toth et al., 2016) – reduced the injury-related neurological deficit (Glushakov et al., 2013). The FP-receptor-linked neurodegenerative signaling is likely Ca^{2+}-dependent, because the agonism of FP receptors increased intracellular Ca^{2+}

concentration in cultured neurons (Kim et al., 2012), although the presence of FP receptors on neuronal membranes have not been unequivocally confirmed. Indeed, the comprehensive localization and distribution of FP receptors in the central nervous system is still to be established.

The synthesis of the experimental results on the implication of PGF2α – FP receptor signaling in ischemic brain injury and SD prompted us to hypothesize that SD must be a central mechanism in FP receptor activation-related ischemic neuronal injury. We postulate that neuronal FP receptors are activated by PGF2α accumulating with SD, which may directly promote neurodegeneration. Simultaneously, cerebrovascular PGF2α – FP receptor signaling in response to SD may potentiate vasoconstriction, and thereby impede neuronal survival under penumbra-like ischemic conditions. To test the hypotheses, we carefully analyzed the characteristics of SD and the coupled CBF response under pharmacological FP receptor antagonism in comparison with control conditions in the ischemic rat brain. Then, the degree of ischemia/reperfusion injury was evaluated with immunocytochemistry in perfusion-fixed brain slices of the animals. Also, we set out to identify which distinct elements of the nervous tissue carry FP receptors, to confirm potential sites of action. Taken together, the ultimate purpose of this study has been to evaluate the protective potential of FP receptor antagonism against SD and the related neurodegeneration.

2. Materials and methods

2.1. Animals

The experimental procedures were approved by the National Food Chain Safety and Animal Health Directorate of Csongrád County, Hungary. The procedures were performed according to the guidelines of the Scientific Committee of Animal Experimentation of the Hungarian Academy of Sciences (updated Law and Regulations on Animal Protection: 40/2013. (II. 14.) Gov. of Hungary), following the EU Directive 2010/63/EU on the protection of experimental animals, and in accordance with the ARRIVE guidelines.

Young adult, male Sprague-Dawley rats (Charles River Laboratories, 342 ± 40 g, $n = 19$) were used in this study. Standard rodent chow and tap water were supplied ad libitum. The animals were housed under constant temperature, humidity, and lighting conditions (23 °C, 12:12 h light/dark cycle, lights on at 7 a.m.).

The designed rate of the two groups (untreated and treated) was 1. The necessary number of animals in each group was at least 7 to support 80% power (β = 20% risk of second species), which was calculated based on the standard deviation of electrophysiological and hemodynamic parameters in earlier studies and the presumed differences between the means of the two groups. The calculations were made in software PS 3.1.2 version (Vanderbilt University, USA) and were also tested in software GPower 3.1 (Heinrich Heine University of Düsseldorf).

2.2. Surgical procedures

Animals were anesthetized with 1.5–2% isoflurane in $N_2O:O_2$ (2:1) and were allowed to breathe spontaneously through a head cone during the experiment. Body temperature was kept at 37.2 °C by a feedback-controlled heating pad (Harvard Apparatus, USA). Atropine was administered (0.1%, 0.05 ml; i.m) as premedication in order to avoid the production of airway mucus. Mean arterial blood pressure (MABP) and heart rate were monitored with a Mikro-Tip pressure catheter inserted to the left femoral artery (Mikro-Tip BP Foundation System, ADInstruments, Australia). The adjacent femoral vein was cannulated for drug administration. The respiratory rate was monitored with a piezo-electric pulse transducer (Pulse Transducer (DIN), ADInstruments, Australia) attached to the chest of the animal. For the later initiation of incomplete global forebrain ischemia, a midline
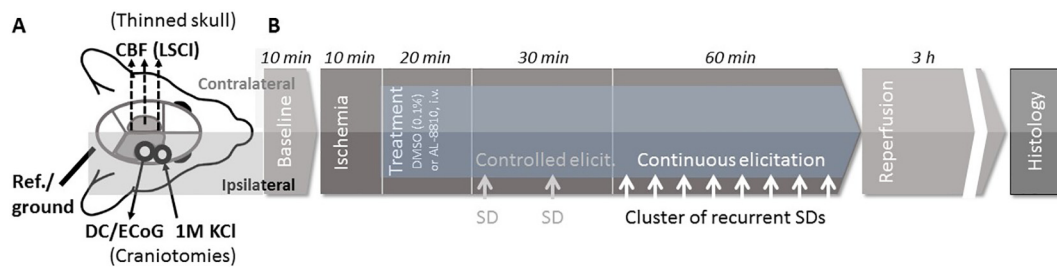
Fig. 1. Graphical illustration of the experimental protocol. A, In the preparation, black circles indicate the position of the two open cranial windows (1 mm caudal from bregma and 5 mm lateral from the sagittal suture), created for the recording of the electrocorticogram (ECoG) and direct current (DC) potential (caudal window) and the experimental elicitation of spreading depolarizations (SD) with KCl (rostral window). The dorsal cranium thinned for the monitoring of cerebral blood flow (CBF) with laser speckle contrast imaging (LSCI) is shaded gray. B, The schematic drawing illustrates the subsequent phases of the experimental protocol. After the initiation of global forebrain ischemia, the FP receptor antagonist AL-8810 or its vehicle, 0.1% dimethyl sulfoxide (DMSO) was bolus injected *i.v.*. Subsequently, SDs were triggered – in a controlled and then a continuous manner – at the ipsilateral cerebral cortex. After a period of reperfusion, the brains were removed for histological examination.

incision was made in the neck and each common carotid artery was carefully looped around with a surgical thread. Lidocaine (1%) was used for local anesthesia. All rats were fixed by their head in a prone position in a stereotaxic apparatus. The scalp was opened, and the temporal muscle was gently retracted from the temporal bones. Two adjacent craniotomies (5 mm lateral from the sagittal suture, −1, −5 caudal from the bregma) were prepared on the right parietal bone with a dental drill (ProLab Basic, Bien Air 810, Switzerland) (Fig. 1). The dura was then carefully opened in each craniotomy. The caudal window was used for electrophysiological monitoring, while the rostral window served SD elicitation. The cranial windows were constantly kept moist by artificial cerebrospinal fluid (aCSF; mM concentrations: 126.6 NaCl, 3 KCl, 1.5 CaCl$_2$, 1.2 MgCl$_2$, 24.5 NaHCO$_3$, 6.7 urea, 3.7 glucose bubbled with 95% O$_2$ and 5% CO$_2$ to achieve a constant pH of 7.4). The rest of the bone was thinned, including the medial part of the contralateral parietal bone (Fig. 1) in order to visualize CBF changes with laser speckle contrast imaging (LSCI) (PeriCam PSI HR, Perimed AB, Sweden).

Two of the rats were excluded because they developed respiratory failure under anesthesia and died as a consequence during the experimental protocol. One additional animal was terminated before the beginning of the experimental protocol because the preparation of the cranial window caused extensive hemorrhage. This resulted in group sizes of 7 and 8 rats, AL-8810-treated and control, respectively.

2.3. Recording of electrophysiological variables and imaging of cerebral blood flow

For the acquisition of the electrocorticogram (ECoG) and slow cortical or direct current (DC) potential, a saline-filled (120 mM NaCl) glass capillary microelectrode (20 μm outer tip diameter) was inserted 700 μm deep into the right somatosensory cortex. An Ag/AgCl reference electrode was implanted under the skin of the animal's neck. The electrophysiological signals were recorded via a high input impedance pre-amplifier (NL102GH, NeuroLog System, Digitimer Ltd., United Kingdom), connected to a differential amplifier (NL106, NeuroLog System, Digitimer Ltd., United Kingdom) with associated filter (ECoG filtered in wideband scale: 0.5–35 Hz, DC filtered in DC mode; < 0.5 Hz) and conditioner systems (NL125, NL144, NL530, NeuroLog System, Digitimer Ltd., United Kingdom). Line frequency noise (50 Hz) was removed by a high-quality noise eliminator (HumBug, Quest Scientific Instruments Inc., Canada). The electrical signals along with MABP and respiration were digitalized by a PowerLab data acquisition device (ADInstruments, Australia) controlled through a dedicated software LabChart 8 (ADInstruments, Australia) at a sampling frequency of 2 kHz.

Laser speckle contrast imaging was used to record SD-associated changes in local CBF over the bilateral somatosensory cortex under

thinned cranial bones. Heatmap images of CBF were created in the software PIMSoft (Software Version 1.3, Perimed AB, Sweden), dedicated to the LSCI apparatus PeriCam PSI HR (Perimed AB, Sweden). Three regions of interest (0.01 mm^2 each) were positioned over the right parietal cortex (posterior, lateral, anterior) ipsilateral to SD induction to extract local CBF variations from the CBF image sequence (Fig. 4A). Arbitrary perfusion units were converted to relative CBF changes offline, with respect to the first 5 min of baseline (100%) and averaged biological zero (0%) taken from previous experiments.

2.4. Experimental protocol

After 10 min of baseline period, both common carotid arteries were occluded (2-vessel occlusion, 2VO) by pulling and securing the surgical threads looped around the vessels. Successful 2VO was confirmed by a sharp drop of CBF. The FP-receptor antagonist AL-8810 (1 mg/bwkg, dissolved in 0.1% dimethyl sulfoxide in physiological saline, Sigma-Aldrich, USA) or its vehicle were bolus administered i.v. in 1 ml volume 10 min after 2VO onset (Fig. 1). The dose of AL-8810 was selected to correspond to a dose found effective to reduce ischemic brain infarct volume in a previous experimental study, where AL-8810 was injected i.v. at 1 or 10 mg/bwkg (Kim et al., 2012). Since the lower concentration was found effective (Kim et al., 2012), and lower drug concentrations are expected to deliver potential side effects less likely, we designed our experiments accordingly. SDs were triggered with a 1 M KCl-soaked cotton ball placed on the cortex (Farkas et al., 2011) 20 min after drug infusion (Fig. 1.). The cotton ball was removed and the craniotomy rinsed with aCSF after two subsequent SD events, provoked at an inter-SD interval of at least 15 min. Next, the KCl-soaked cotton ball was left on the brain surface for 60 min to induce clusters of SDs. Finally, reperfusion was initiated by releasing the carotid arteries, and the animals were kept under light sedation (1% isoflurane) for an additional 3 h in order for ischemic tissue injury to mature.

2.5. Tissue processing and immunocytochemistry

The animals were transcardially perfused with ice-cold physiological saline followed by 4% paraformaldehyde (PFA) under deep chloral hydrate anesthesia (5%, i.p., 500 mg/bwkg) at the end of the experimental protocol. The brains were removed, stored in 4% PFA at 4 °C overnight, and cryoprotected in 30% sucrose in phosphate buffered saline (PBS). Coronal, 20-μm-thick forebrain sections were cut with a freezing microtome (Leica CM 1860 UV, Leica, Germany). Slices were selected for the permanent immunocytochemical staining of cleaved caspase-3 (CC3), the immunofluorescent co-localization of CC3 with the neuron marker neuronal nuclear protein (NeuN) or the astrocyte marker glial fibrillary acidic protein (GFAP), or the immunofluorescent co-localization of FP receptors with neural glial, as well as

cerebrovascular elements.

First, apoptotic cell injury was characterized with cleaved caspase-3 (CC3) and the activation of microglia with ionized calcium-binding adapter molecule (Iba1) immunolabeling on selected coronal slices (bregma +1, −3.14 and −6.04 mm, Paxinos and Watson atlas co-ordinates; two slices per plane). Endogenous peroxidases were blocked with 5% H_2O_2, nonspecific protein-binding sites were blocked with 5% normal goat serum (Merck, Kenilworth, USA), and slices were permeabilized with 0.5% Triton X-100 (Merck, Kenilworth, USA) in Tris-buffered saline (TBS). Slices were incubated with rabbit anti-CC3 or anti-Iba1 primary antibody (CC3: Abcam, ab13847, 1:300; Iba1: rabbit, FujiFilm Wako, NCNP24, 1:3000) overnight at 4 ˚C. The subsequent steps of incubation included an enhancer reagent for 1 h at room temperature, and horseradish-peroxidase-linked secondary antibody for 3 h at room temperature, both being components of the Polink-2 Plus HRP Detection Kit (for rabbit primary antibody with diaminobenzidine (DAB) chromogen, D39–18, GBI Labs, USA). The staining was visualized with DAB. The slices were mounted on microscopic slides with Eukit® (Merck, USA) and digitally recorded either with a microscope slide scanner (Zeiss Mirax Midi Slide Scanner, Carl Zeiss MicroImaging GmbH, Germany) operated by a CaseViewer software (3D Histech Ltd., Hungary), or a Nikon-DS Fi3 camera attached to a Leica DM 2000 Led light microscope (Leica Microsystems GmbH, Germany). The CC3-labeled slides were evaluated by manual cell counting with the CellCounter plugin of ImageJ by two observers blind to the experimental design (Wayne Rasband, NIH). In the Iba1-immunolabeled slices, cells were counted, and microglia activation was characterized with a ramification index exactly as reported earlier (Tóth, 2020)

Next, the cell types of the nervous tissue involved in apoptotic cell death were identified by the representative co-localization of cleaved caspase-3 with NeuN or GFAP. Antigens were retrieved with 10-minute-long boiling in citrate buffer (pH 5, 95 ˚C, 300 rpm). Slices were permeabilized with 0.2% Triton X-100 in PBS for 30 min. Non-specific protein-binding sites were blocked with 3% bovine serum albumin (BSA) for 1 h at room temperature. Slices were incubated with primary antibodies overnight at 4 ˚C (anti-cleaved caspase-3: rabbit, Cell Signaling, #9661, 1:500; anti-GFAP: mouse, Sigma, G3893, 1:10000; anti-NeuN: mouse, Millipore, MAB377, 1:500; in 1% BSA in PBS). Secondary antibodies were applied for 1 h at room temperature (anti-rabbit Alexa 594; goat, Jackson Laboratories, 1:500; anti-mouse Alexa 488, goat, Jackson Laboratories, 1:500; in 1% BSA in PBS). Slices were mounted with Fluoromount-G with DAPI (Thermo Fisher Scientific, USA), for the additional visualization of cell nuclei. Representative photomicrographs were taken of the somatosensory cortex of a control animal with a Leica SP5 inverted laser scanning confocal microscope (TE2000U, Leica Microsystems GmbH, Germany) with 63× objective with additional digital zoom giving. Confocal images were pieced together and processed in ImageJ.

Finally, in order to identify the cellular and subcellular localization of FP receptors, the receptors were co-labeled with NeuN (neuronal marker), GFAP (astrocyte marker), Iba1 (microglia marker), claudin-5

(endothelial cell marker) or alpha-actin (vascular smooth muscle cell marker) in slices from a naïve animal. Antigens were retrieved with 10-minute-long boiling in citrate buffer (pH 5; 95 ˚C, shaking at 300 rpm) for claudin-5 co-staining. All slices were permeabilized with 0.2% Triton X-100 in PBS for 30 min. Non-specific protein-binding sites were blocked with 3% BSA for 1 h at room temperature. Slices were incubated with primary antibodies overnight at 4 ˚C (anti-FP receptor: rabbit, Abcam, ab203342, 1:100; anti-NeuN: mouse, Millipore, MAB377, 1:500; anti-GFAP: mouse, Sigma, G3893, 1:10000; anti-Iba-1: goat, Abcam, ab48004, 1:500; anti-claudin-5: mouse, Invitrogen, #4C3C2, 1:100; in 1% BSA in PBS; anti-α-smooth muscle actin, GeneTex, GTX73419, ready-to-use). Secondary antibodies were applied for 1 h at room temperature (anti-rabbit STAR RED; goat, Abberior, 1:500; anti-mouse STAR 580, goat, Abberior, 1:500; anti-goat Alexa-594, donkey, Thermo Fisher Scientific, 1:500; in 1% BSA in PBS). In case of Iba-1 and FP double staining, the incubation with anti-goat secondary antibody was followed by the incubation with goat anti-rabbit antibody to avoid cross-reaction. Slices were mounted with Fluoromount-G (Thermo Fisher Scientific). Representative confocal images were taken of the somatosensory cortex with a Zeiss Axio Observer Z1 inverted microscope (Carl Zeiss GmbH, Germany), and pieced together and processed in ImageJ (National Institutes of Health, Bethesda, Maryland, USA).

2.6. Data analysis

Physiological variables (i.e. DC potential and MABP) were simultaneously acquired, displayed live, and stored using a personal computer equipped with the software LabChart 8 (ADInstruments, Australia). the LSCI signal was acquired with PeriFlux System 5000 (Perimed AB, Sweden) and displayed live with PIMSoft. Raw LSCI recordings were downsampled to 1 Hz before analysis. All data were then converted and analyzed with the inbuilt instructions of the software AcqKnowledge 4.2 for MP 150 (Biopac Systems, Inc., USA).

Blinding data analysis was intended by assigning codes to files and recordings, which do not reveal the experimental condition (i.e., date of the experiment). The SD events were first sorted according to their duration and amplitude: With reference to regular transient SDs, prolonged SDs were noted when the depolarization was longer than 3 min while the amplitude of the depolarization was similar to transient SDs (> 10 mV), and incomplete SDs were identified by their amplitude smaller than 10 mV, and their duration shorter than 30 s (Fig. 2A). For all SD events, peak amplitude, duration at half amplitude, the rate of depolarization and repolarization, and area under the curve (AUC) were measured on the DC potential trace. The distribution of spectral power of the ECoG recordings at alpha (8–13 Hz) and delta (1–4 Hz) frequency bands were done with the software LabChart Pro (Labchart 8, National Instrument, Australia). Total power for each frequency band was expressed for 60-s periods taken (i) before the induction of cerebral ischemia, (ii) before the controlled elicitation of the 1st SD, (iii) before continuous SD elicitation, and (iv) after reperfusion. As a proxy for
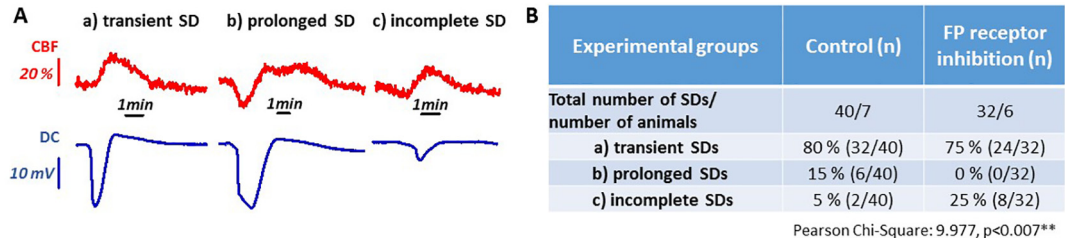

Experimental groups	Control (n)	FP receptor inhibition (n)
Total number of SDs/ number of animals	40/7	32/6
a) transient SDs	80 % (32/40)	75 % (24/32)
b) prolonged SDs	15 % (6/40)	0 % (0/32)
c) incomplete SDs	5 % (2/40)	25 % (8/32)

Pearson Chi-Square: 9.977, p<0.007**

Fig. 2. Distinct types of spreading depolarization (SD) events, and their incidence during the phase of continuous elicitation. A, Traces depict DC potential changes (lower trace, blue) and cerebral blood flow (CBF) responses (upper trace, red) representative of the different types of SDs. B, The incidence of various SD types are given relative to the total number of SDs for the two experimental groups. Statistical association between Treatment and Types of SDs was analyzed with Chi-Square Test (p = .01**). (For interpretation of the references to colour in this figure legend, the reader is referred to the web version of this article.)

latter lesion formation, alpha-to-delta ratio (ADR) was calculated for each time points (Menyhárt et al., 2015). SD frequency was also calculated for recurrent events under continuous elicitation.

The CBF response to SD was first categorized as hyperemic (dominating element of transient hyperemia), hypoemic (transient hypoperfusion alone) or no detectable CBF variation at a clear negative shift (i.e. > 10 mV) of the DC potential (Bere et al., 2014). The SD-associated hyperemia and hypoemia were then characterized by the peak amplitude, and the duration of the transient CBF change. Data analysis was shared among four independent investigators.

Data are given as mean $\pm$ stdev; parametric data are shown as bar charts, while non-parametric data are presented with additional scatter plots. The results were statistically analyzed with the software SPSS (IBM SPSS Statistics for Windows, Version 22.0, IBM Corp.). Grubbs test was applied to identify potential outliers. For the evaluation of statistical significance, a repeated measure or a two-way analysis of variance (ANOVA) model was used for data sets with normal distribution. Tukey's HSD or Games–Howell post hoc test was used for group comparisons, whenever applicable. When the data did not fit normal distribution, non-parametric Mann-Whitney test was used. Frequency distributions were evaluated with a Pearson's Chi-square test. Levels of significance were defined as $p < .05*$ and $p < .01**$. All relevant statistical methods are given in each figure legend.

3. Results

3.1. Physiological parameters were unaltered by the AL-8810 treatment

In order to evaluate whether the intravenous administration of AL-8810 had any potential impact on systemic physiological variables, we analyzed arterial blood samples and cardiorespiratory parameters (Table 1). The systemic physiological variables were within the normal range throughout the experimental protocol. Ischemia increased MABP (e.g. vehicle group: 85.3 $\pm$ 10.5 vs. 78.0 $\pm$ 9.3 mmHg, ischemia vs. baseline) and arterial pO_2 (e.g. vehicle group: 110.9 $\pm$ 11.8 vs. 105.4 $\pm$ 15.1 mmHg, ischemia vs. baseline), as in other experimental models of cerebral ischemia (Menyhárt et al., 2015; Lückl et al., 2018). The treatment with AL-8810 did not exert any detectable impact on the examined variables (Table 1).

3.2. AL-8810 reduced depolarization time and promoted early recovery after SD

The occurrence of SD clusters or prolonged depolarizations, and the long cumulative duration of recurrent SDs indicate and predict the development of secondary ischemic brain injury after an acute insult (Dreier et al., 2006; Hartings et al., 2017a; Shuttleworth et al., 2019). We have demonstrated earlier that the inhibition of the EP4 receptor of PGE2 causes the unfavorable elongation of SD in the ischemic cerebral cortex (Varga et al., 2016). Here we explored whether the antagonism of the FP receptor of PGF2α modulates the occurrence or duration of SDs beneficially.

SD occurrence was confirmed with electrophysiology and LSCI in the ipsilateral cortex, but no SD propagation to the contralateral side was seen in the CBF maps. In case of the initial, controlled elicitation, all SDs were transient with no statistical difference in the DC potential signature between the two groups (i.e. amplitude: −18.3 $\pm$ 2.7 vs. −18.0 $\pm$ 2.6 mV, AL-8810 vs. vehicle; duration at half amplitude: 55 $\pm$ 25 vs. 56 $\pm$ 19 s, AL-8810 vs. vehicle).

Subsequent to controlled SD elicitation, clusters of SDs were triggered with continuous KCl exposure. Each of these recurrent SDs was categorized as transient, prolonged or incomplete, on the basis of their DC potential signature acquired at the implanted electrode (Fig. 2A). Then their incidence relative to the total number of recurrent SDs was expressed for the AL-8810 and the vehicle-treated groups separately (Fig. 2B). Incomplete SDs typically occurred towards the end of the continuous SD elicitation. The antagonism of FP receptors with AL-8810 prevented the evolution of prolonged SDs (0 vs. 15%, AL-8810 vs. vehicle), and achieved a complementary increase in the incidence of incomplete SDs (25 vs. 5%, AL-8810 vs. vehicle). At the same time, the share of regular transient SDs of all recurrent events remained comparable between the two experimental groups (75 vs. 80%, AL-8810 vs. vehicle) (Fig. 2B).

Detailed, quantitative analysis of recurrent SDs focused on transient events (Fig. 3). Similar to the controlled SDs, the amplitude of the clustered SDs was similar in the two experimental groups (−17.5 $\pm$ 2.4 vs. −16.9 $\pm$ 3.1 mV, AL-8810 vs. vehicle). Nevertheless, AL-8810 treatment accelerated the repolarization after SDs (0.84 $\pm$ 0.4 vs. 0.45 $\pm$ 0.22 mV/s, AL-8810 and vehicle) (Fig $3A_1$). Accordingly, the average duration of an SD at half amplitude (30 $\pm$ 10 vs. 56 $\pm$ 14 s, AL-8810 vs. vehicle) (Fig. $3A_2$), as well as the cumulative duration of recurrent transient SDs was found shorter (304 $\pm$ 71 vs. 577 $\pm$ 154 s, AL-8810 vs. vehicle) in the AL-8810-treated compared to the control group. In line with these data, the magnitude of individual SDs expressed as AUC was reduced in the AL-8810 treated group compared to control (585 $\pm$ 192 vs. 942 $\pm$ 251 mV*s; AL-8810 vs. vehicle) (Fig $3A_3$). Taken together, FP receptor blockade prevented the development of prolonged depolarization, accelerated repolarization, and shortened the cumulative duration of clustered, recurrent SDs.

3.3. AL-8810 increased electrocorticographic alpha-to-delta ratio in the reperfused cortex

Lowering electrocorticographic alpha-to-delta ratio (alpha power/ delta power, ADR) has been proposed as a sensitive and selective tool to predict the evolution of delayed cerebral ischemia after aneurismal subarachnoid hemorrhage (Claassen et al., 2004; Rots et al., 2016; Yu et al., 2019). In addition, delayed cerebral ischemia has been linked to SD (Dreier et al., 2006; Dreier et al., 2009). Therefore, we calculated ECoG power for alpha (8–13 Hz) and delta (1–4 Hz) frequency bands and expressed ADR for 4 selected time points over the experimental protocol (Fig. $3B_1$). As expected, ADR taken prior to ischemia induction and the initiation of AL-8810 treatment was comparable for the two experimental groups (0.67 $\pm$ 0.20 and 0.63 $\pm$ 0.29; AL-8810 and vehicle). ADR remained similar 30 min after the induction of ischemia and the administration of AL-8810 (0.81 $\pm$ 0.36 and 0.65 $\pm$ 0.26; AL-

Table 1
Physiological variables.

Pharmacological treatment	n	Body weight (g)	Time of sampling	MABP (mmHg)	Heart rate (BPM)	Rate of respiration (Hz)	Arterial pO_2 (mmHg)	Arterial pCO_2 (mmHg)
Vehicle	8	335 $\pm$ 48	Before 2VO	78.0 $\pm$ 9.3	352 $\pm$ 49	1.19 $\pm$ 0.12	105.4 $\pm$ 15.1	41.6 $\pm$ 3.2
			After 2VO	85.3 $\pm$ 10.5*	328 $\pm$ 58	1.12 $\pm$ 0.13	110.9 $\pm$ 11.8*	38.4 $\pm$ 7.2
AL-8810	7	353 $\pm$ 38	Before 2VO	78.1 $\pm$ 7.7	339 $\pm$ 22	1.31 $\pm$ 0.19	102.6 $\pm$ 16.1	38.5 $\pm$ 3.0
			After 2VO	83.5 $\pm$ 8.5*	334 $\pm$ 28	1.22 $\pm$ 0.24	118.6 $\pm$ 27*	38.6 $\pm$ 2.3

Data are given as mean $\pm$ stdev. A two-way ANOVA model (factors: ischemia and treatment) was used for statistical analysis. Ischemia was found to increase blood pressure and arterial pO_2 significantly (p < .05*). Abbreviations: 2VO, permanent, bilateral occlusion of the common carotid arteries ("two-vessel occlusion"); BPM, beat per minute; MABP: mean arterial blood pressure.
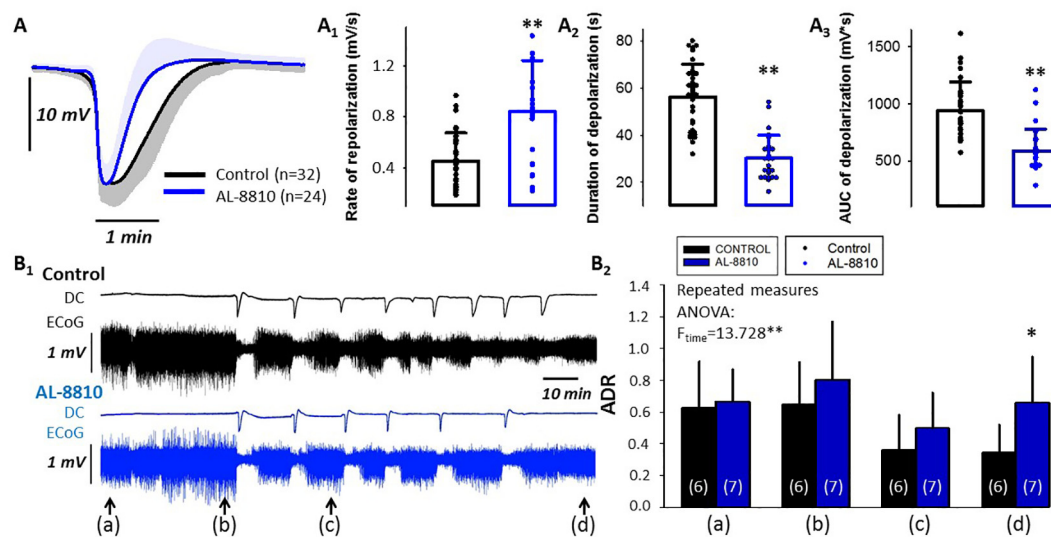
Fig. 3. The impact of AL-8810 treatment on the electrophysiological features of spreading depolarization (SD). A, The transient, negative DC potential shift indicating SDs, triggered under continuous elicitation, is shown for each group (mean ± stdev). The rate of repolarization (A_1), the duration at half amplitude (A_2) and the area under the curve (AUC) (A_3) of the negative DC potential shift are depicted in bar charts. Dots denote individual values. Statistical analysis relied on Mann-Whitney Rank sum test; **$p < .01$. B_1, Representative DC potential traces and the corresponding electrocorticogram (ECoG) of a control (black) and an AL-8810 (blue) treated animal. Note the typical depression of the ECoG with each SD. The ratio of the power of the frequency bands alpha and delta (alpha/delta ratio, ADR) was calculated before the induction of cerebral ischemia (a), before the controlled elicitation of the 1st SD (b), before continuous SD elicitation (c), and after reperfusion initiation (d). B_2, ADR for the selected segments of the ECoG recordings. Statistical comparison relied on a repeated measures ANOVA (factor: treatment; p < .01**). Pairwise comparisons for each time point were conducted with one-way ANOVA; *$p < .05$, AL-8810 vs. respective control. Sample size is indicated in each bar. (For interpretation of the references to colour in this figure legend, the reader is referred to the web version of this article.)

8810 and vehicle). After the controlled elicitation of two SDs, ADR reduced in both experimental groups equally (0.45 ± 0.23 and 0.36 ± 0.22; AL-8810 and vehicle). Finally, 5 min after the initiation of reperfusion and the cessation of clusters of recurrent SDs, ADR increased selectively in the AL-8810 treated group (0.66 ± 0.29 vs. 0.35 ± 0.17; AL-8810 vs. vehicle) (Fig. 3B_2). Thus, ADR – a perceived predictor of late ischemic injury – was improved during early reperfusion by AL-8810 treatment.

3.4. AL-8810 augmented hyperemia and attenuated hypoperfusion with SD

The CBF response to SD consists of at least three distinct elements including a brief, early hypoperfusion, a subsequent, substantial hyperemia, and a final, long lasting oligemia (Ayata and Lauritzen, 2015). The pharmacological augmentation of the CBF response to SD in the service of neuroprotection is a realistic goal, because insufficient hyperemia and especially the occurrence of spreading ischemia (i.e. the early hypoperfusion element of the CBF response overriding the hyperemic component) delays repolarization and reduces the viability of penumbra tissue (Dreier, 2011; Hartings et al., 2017a).

The spatial resolution offered by LSCI in our experiments enabled a comprehensive analysis of the CBF response to SD. We concentrated our detailed analysis on recurrent SDs, which emerged as regular, transient negative DC potential shifts (amplitude > 10 mV, duration < 3 min) at the electrode implanted. First, with the aid of placing multiple regions of interest (ROIs) on the CBF videos (Fig. 4A), we noted that the kinetics of the CBF response associated to a given SD may alter over the course of SD propagation. Hyperemic CBF response was most frequently encountered at the ROI positioned over the open cranial window incorporating the electrode (lateral in Fig. 4A–C; 92 and 100%, AL-8810 and vehicle). The CBF response to the same SD often escaped detection ("no CBF response") at ROIs over the thinned parietal bone (anterior: 31 and 48%, posterior: 35 and 26%, AL-8810 and vehicle). Finally, the CBF response transformed occasionally to hypoperfusion at the anterior ROI placed over the medial fronto-parietal cortex, particularly in the control group (12 and 22%, AL-8810 and vehicle) (Fig. 4A–B).

The detailed, quantitative analysis of the hyperemic CBF responses revealed that AL-8810-treatment elevated baseline CBF prior to SD (e.g. lateral ROI: 73.0 ± 13.8 vs. 56.8 ± 6.3%; AL-8810 vs. vehicle), and therefore augmented the absolute amplitude of the SD-coupled hyperemia, as well (e.g. lateral ROI: 104.1 ± 25.0 vs. 76.0 ± 8.6%, AL-8810 vs. vehicle) (Fig. 4D). Further, AL-8810 treatment attenuated hypoemic CBF responses, which was reflected by the smaller relative amplitude of the hypoperfusion transients (−5.4 ± 1.7 vs −14.0 ± 1.8 pp., AL-8810 vs. vehicle) (Fig. 4E). Also, progressive perfusion deficit during continuous SD elicitation was less prominent in the AL-8810 treated group compared to control, resulting in higher CBF prior to the initiation of reperfusion (68.2 ± 14.5 vs. 58.6 ± 9.6%, AL-8810 vs. vehicle). Finally, the rate of propagation of the SD coupled CBF response was accelerated under AL-8810 treatment compared to the control condition (3.0 ± 0.7 vs. 2.4 ± 0.5 mm/min, AL-8810 vs. vehicle) (Fig. 4F). Together these data demonstrate that AL-8810 treatment increased CBF in the ischemic cerebral cortex, and counteracted transient CBF reduction with SD.

3.5. AL-8810 treatment salvaged SD triggered apoptosis in the cortex, but exerted no impact on microglia activation

Cleaved caspase-3 (CC3) has been a widely accepted apoptosis marker in the nervous tissue (Fricker et al., 2018), which can be detected confidently 3 h after the onset of reperfusion (Davoli et al., 2002; Manabat et al., 2003).

Accordingly, we collected brain samples 3 h after the initiation of reperfusion to assess the neuroprotective potential of AL-8810. CC3-positive apoptotic cells were observed in striatal, hippocampal and cortical areas in both experimental groups, albeit to a lesser degree in the AL-8810-treated animals (Fig. 5A-B_1). The immunofluorescent co-localization of CC3 with NeuN and GFAP revealed that both neurons and astrocytes were engaged in apoptosis (Fig. 5B_2). With the anticipation of more extensive apoptosis in the hemisphere ipsilateral to SD elicitation, the number of CC3-immunopositive cells was normalized to the contralateral side. The quantitative approach suggested a significant
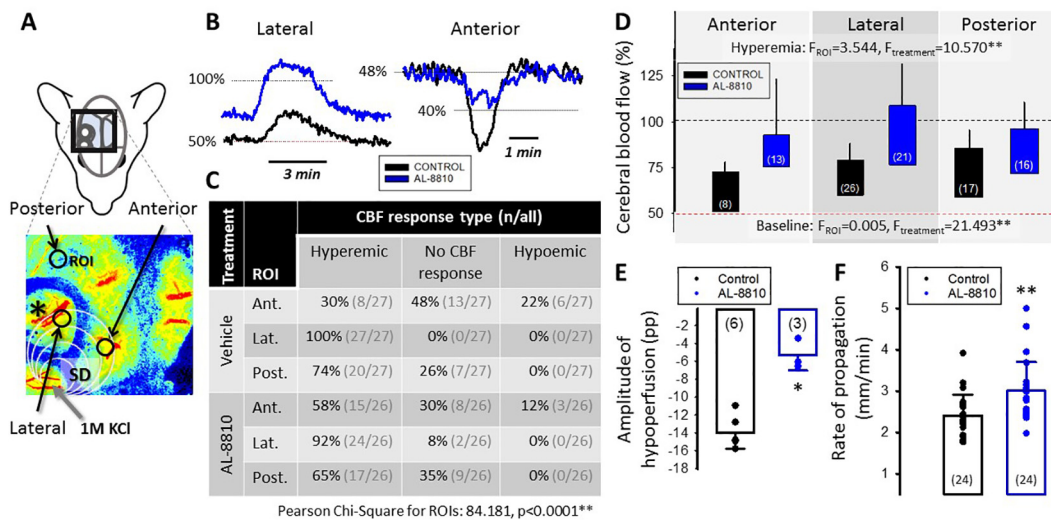
Fig. 4. The impact of AL-8810 treatment on the cerebral blood flow (CBF) response to spreading depolarization (SD) under continuous elicitation. A, A representative CBF map obtained with laser speckle contrast imaging demonstrates the 3 regions of interest (ROI), at which CBF variations were extracted: the lateral, the anterior, and the posterior parietal cortex. The asterisk denotes the position of the glass capillary electrode implanted. B, Representative hyperemic and hypoemic CBF responses to SD recorded from a control (black) and an AL-8810 treated (blue) animal. C, The table gives an overview of the occurrence of CBF response types relative to all events at the distinct ROIs in the two experimental groups. Statistical association between ROI position and CBF response type was analyzed with a Pearson Chi-Square Test ($p < .01**$). D, Baseline CBF prior to SD occurrence and the absolute amplitude of peak hyperemia coupled to SD in the anterior, lateral and posterior parietal cortex. The base of each bar is set to the CBF level preceding the SD events. E, The relative amplitude of hypoperfusion. F, The average rate of propagation of SDs calculated from the CBF maps for each group. Data in D-F are given as mean ± stdev; spherical symbols in E-F represent individual values. Statistical analysis relied on a repeated ANOVA (D) or Mann-Whitney Rank sum test (E–F); $p < .05*$ and $p < .01**$. The number of events analyzed is indicated in each bar. (For interpretation of the references to colour in this figure legend, the reader is referred to the web version of this article.)
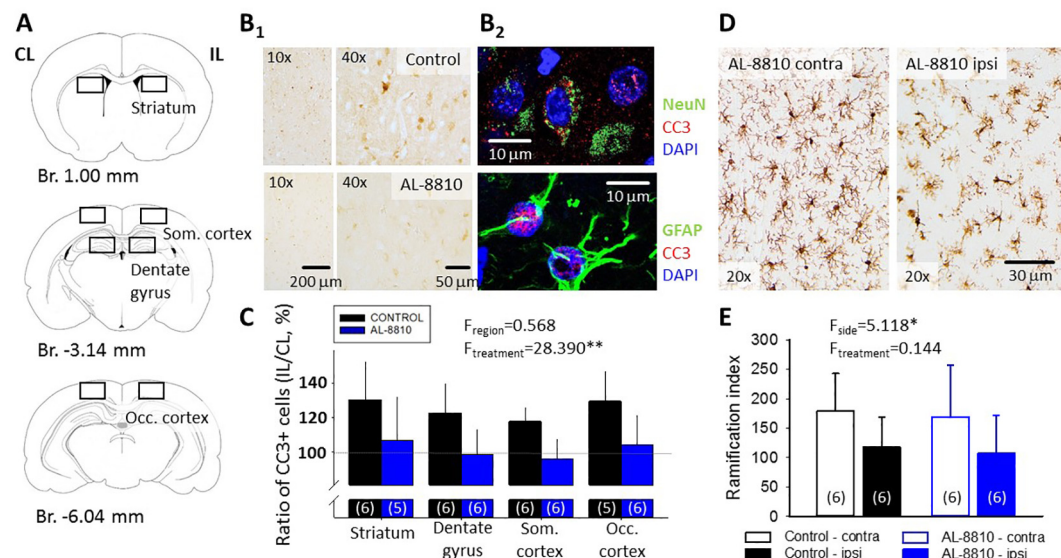

Fig. 5. Neuroprotection achieved by FP receptor antagonism in the rat brain. A, Schematic coronal brain slices demonstrate gray matter regions in the ipsilateral (IL, spreading depolarization elicitation on the background of ischemia) and contralateral (CL, ischemia alone) brain hemispheres, in which cleaved caspase-3 (CC3) positive, apoptotic cells were quantitated: the striatum, the dentate gyrus of the hippocampus, and somatosensory parietal and occipital cortical areas (Som. and Occ. cortex, respectively). B₁, Representative photomicrographs taken of the occipital cortex ipsilateral to SD elicitation demonstrate that the number of CC3-labeled cells (chromogen: diaminobenzidine) was reduced in the AL-8810-treated group compared to the control condition. B₂, Fluorescent co-localization of CC3 labelling with the cell nuclei (DAPI) of NeuN positive neurons (top) or GFAP-positive astrocytes (bottom) revealed that both neurons and astrocytes were engaged in apoptosis. C, The CC3-positive cell count demonstrated that apoptosis was more prevalent in the hemisphere ipsilateral to SD elicitation, relative to the contralateral side. AL-8810 proved to exert neuroprotection in that the number of CC3-positive cells was similar in the two hemispheres in the treated group, particularly in the dentate gyrus and the cerebral cortex. Data are given as mean ± stdev; sample size is given in each bar; statistical analysis was conducted using repeated measures ANOVA with treatment as a factor ($**p < .01$). D, Representative images of Iba1 immunolabeled microglia. Photomicrographs were taken of the somatosensory cortex at −3.14 mm from bregma. E, Microglial activation represented by the ramification of microglia was augmented in the ipsilateral compared to the contralateral cerebral cortex, irrespective of treatment. Data are given as mean ± stdev; sample size is given in each bar; statistical analysis was conducted using a two-way ANOVA model with lateralization and treatment as factors ($*p < .05$).

neuroprotective effect of AL-8810 shown by the reduction of CC3 positive cell numbers in the ipsilateral relative to the contralateral hemisphere (e.g. somatosensory and occipital cortices: 94.4 ± 12.6% vs. 112.9 ± 7.0%; 104.3 ± 17.6% vs. 125,7 ± 17,7%, respectively, AL-8810 vs. vehicle) (Fig. 5C). Overall, AL-8810 treatment appeared to offer detectable neuroprotection measured early after ischemia/reperfusion induction.

Microgia activation is a rapid neuro-inflammatory response to injury, which was previously suppressed with AL-8810, assessed days after experimental traumatic brain injury (Glushakov et al., 2013). We have observed intensive Iba1 immuno-labeling in the tissue samples (Fig. 5D). While the number of labeled microglia was similar in the two hemispheres irrespective of treatment (31 ± 7 and 28 ± 6, contra- and ipsilateral), their arborization was less dense in the ipsilateral hemisphere indicative of their increased activation (ramification index: 112.7 ± 55.4 vs. 174.2 ± 73.8, ipsi- vs. contralateral). The administration of AL-8810 did not exert any discernable impact on the ramification of microglia processes (ramification index: 148.6 ± 63.8 and 138.3 ± 80.3, control and AL-8810) (Fig. 5D-E).

3.6. FP receptors were associated with neurons, astrocytes, microglia, and cerebrovascular endothelial cells

FP receptors have been previously identified in brain synaptosomes and microvessels in newborn and adult pigs (Li et al., 1993, 1994), and cultured rat astrocytes (Kitanaka et al., 1994). Here we set out to visualize FP receptor presence on neuronal, glial (astrocyte and microglia) and cerebrovascular (endothelial and smooth muscle cell) compartments as potential sites of AL-8810 action.

The co-localization of FP receptors with NeuN and GFAP confirmed the localization of FP receptors predominantly in the nuclear envelope of neurons (Fig. 6A), as well as in the perikaryon and perivascular endfeet of astrocytes (Fig. 6B₁₋₂). In addition, we observed a robust co-localization of FP receptors with Iba1-labeled microglia (Fig. 6C). The presence of FP receptors was also obvious in claudin-labeled cerebromicrovascular endothelial cells. However, we were not able to detect FP receptors unequivocally in α-actin-labeled cerebrovascular smooth muscle cells. In summary, FP receptor expression has been confirmed in both neuronal, glial and vascular elements in the rat brain.

4. Discussion

Here we have explored the neuroprotective potential of the antagonism of the PGF2α FP receptor in experimental global forebrain ischemia/reperfusion exacerbated by recurrent SDs.

Prostaglandin signaling has been in the center of pharmaceutical research for decades. Importantly, experimental research suggested that cyclooxygenase-2 enzyme (COX-2) inhibition may have therapeutic potential in stroke (Candelario-Jalil and Fiebich, 2008). However, the controversial action of repetitively administered COX-2 inhibitors on platelet function may manifest in cardiovascular adverse effects including thrombus formation and heart failure (Santilli et al., 2016). In particular, in the context of ischemic brain injury, the use of COX-2 inhibitors prior to the occurrence of ischemic stroke was associated with worse stroke outcome in patients (Schmidt et al., 2014). Since COX-2 inhibition suppresses the synthesis of all types of prostaglandins downstream to the enzyme (e.g. PGE2, PGF2α, thromboxanes), and each prostaglandin may act on a number of receptor types mediating complementary or opposing actions, subsequent efforts focused on the selective modulation of distinct prostaglandin receptors. Indeed, the EP1-EP4 receptors of PGE2 have been intensively studied and a wealth of experimental data on their implication in ischemic brain injury have been gathered (Andreasson, 2010). In the context of SD, EP4 receptors appeared to be involved in the repolarization phase of SD in the ischemic rodent brain (Varga et al., 2016). Yet, the FP receptor of PGF2α appears to have received considerably less attention (Zhang et al., 2010; Sharif and Klimko, 2019), even though PGF2α concentration was elevated in the brain tissue and the cerebrospinal fluid in animal models of cerebral ischemia or SD (Gaudet and Levine, 1980; Katz et al., 1988; Shibata et al., 1992), and PGF2α immunolabeling was found enhanced after cerebral ischemia/reperfusion in the cerebral vascular wall and hippocampal neurons of rats (Ogawa et al., 1987).

Our data demonstrate that the antagonism of the PGF2α FP receptors suppressed SD in the ischemic rat cerebral cortex (Fig. 2), reduced the duration of recurrent SDs by facilitating repolarization, and augmented the recovery of ECoG during reperfusion (Fig. 3). Parallel with the neurophysiological actions, FP receptor antagonism improved perfusion in the ischemic cerebral cortex, and attenuated hypoemic CBF responses associated with SD (Fig. 4). Further, FP receptor antagonism appeared to curtail apoptotic cell death related to SD recurrence (Fig. 5). Collectively, these findings are in agreement with a number of previous reports of a research group, which presented that the pharmacological antagonism or genetic knock-out of FP receptors reduced ischemic infarct volume and improved functional outcome in preclinical models of ischemic or traumatic brain injury (Saleem et al., 2009; Kim et al., 2012; Glushakov et al., 2013). Since spontaneous, recurrent SDs of long cumulative duration have been strongly implicated in the pathophysiology of ischemic or traumatic brain injury (Dreier et al., 2006; Hartings et al., 2017a), it is plausible that the facilitated recovery from SD achieved with FP receptor antagonism – as
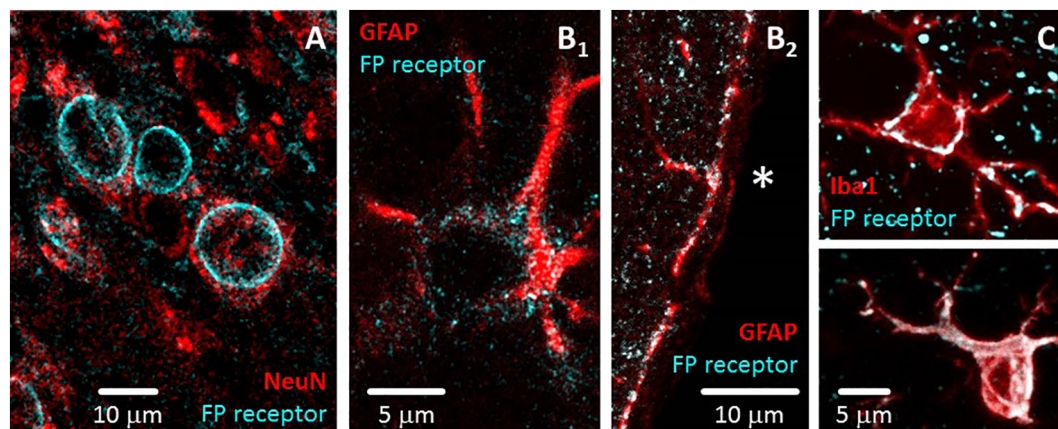

Fig. 6. The cellular localization of FP receptors in the rat brain in representative fluorescent confocal microscopic images. A, FP receptors are associated to the nuclear envelope of neuronal nuclear protein (NeuN)- positive neurons, B₁, FP receptors are localized in the cytoplasm of astrocytes labeled with glial fibrillary acidic protein (GFAP). B₂, FP receptors are seen on GFAP-positive perivascular astrocytic endfeet. The vascular lumen is labeled with an asterisk. C, The co-localization of FP receptors with the microglia marker ionized calcium-binding adapter molecule (Iba1).

shown here – could have contributed to reduced lesion volume and less severe functional deficit registered in the previous studies.

The ability of the nervous tissue to repolarize after SD is subject to the metabolic status of the brain region involved in SD evolution. The increasing severity of ischemia – and thus energy depletion of the tissue – leads to sodium pump dysfunction and the failure of active ion translocation between the intra- and extracellular compartments, and delays the recovery of the resting membrane potential once SD has occurred (Dreier, 2011). Since FP receptor antagonism in our experiments markedly improved the perfusion of the ischemic cerebral cortex (Fig. 4), it is conceivable that SD duration was shortened in the AL-8810-treated animals (Fig. 3) because the tissue was metabolically less compromised. Indeed, FP receptors at the periphery have been previously implicated in the regulation of vascular tone (Zhang et al., 2010). FP receptors were associated with cultured smooth muscle cells of a cell line derived from the embryonic rat aorta (Rice et al., 2008), and the smooth muscle cells of preglomerular arterioles in the kidney (Yu et al., 2009). The presence of FP receptors on vascular smooth muscle cells was suggested to be the anatomical basis for FP receptor linked vasoconstriction (Zhang et al., 2010). In addition to vascular smooth muscle cells, venous endothelial cells of the peripheral vascular network were also found to express FP receptors, which mediated PGF2α-related vasorelaxation of the jugular and submental veins or constriction of the human umbilical vein (Chen et al., 1995; Astin and Stjernschantz, 1997; Zannoni et al., 2007). Finally, membranes prepared from porcine cerebral microvessels were shown to host FP receptors (Li et al., 1994), and PGF2α applied to baboon isolated middle cerebral artery rings was demonstrated to cause dilation at lower, and constriction at higher concentration (Hayashi et al., 1985). We have identified FP receptors associated with endothelial cells and perivascular astrocytic endfeet of the neurovascular unit (Fig. 6), located at an ideal position to contribute to cerebrovascular tone adjustment. Considering the experimental data accumulated on PGF2α-FP receptor signaling in various vascular domains (Zhang et al., 2010), AL-8810 treatment in our study is suggested to have targeted – in part – the FP receptors identified at elements of the neurovascular unit (Fig. 6). FP receptor antagonism with AL-8810 presumably counteracted PGF2α-linked vasoconstrictive tone, and, consequently, improved cerebrocortical blood flow (Fig. 4).

Spreading ischemia coupled to SD that propagates across vulnerable penumbra tissue has been considered particularly harmful (Dreier et al., 1998; Dreier, 2011; Hartings et al., 2017a). We have observed a few events of spreading ischemia near the site of SD elicitation, which transformed to hyperemic CBF response along the direction of SD propagation, with the increasing distance from the SD focus (Fig. 4B). Spreading ischemia occurred near the site of SD elicitation possibly because of the close proximity of the local administration of high concentration KCl to evoke SDs, which has been shown to potentiate SD-related hypoperfusion (Menyhárt et al., 2018). The occurrence of spreading ischemia was less frequent under AL-8810 treatment, and flow reduction with the observed events in the AL-8810 group was considerably attenuated (Fig. 4E). This is considered as additional evidence for the vasoconstrictive role cerebrovascular FP receptors may fulfill in the mediation of the CBF response to SD.

The pharmacological inhibition of the FP receptors in our experiments could have contributed to neuroprotection (Fig. 5) by targeting neurons directly, as well. We have observed conspicuous FP receptor labeling co-localized with neurons (Fig. 6A), which is consistent with previous work that revealed the presence of FP receptors in synaptosome preparations or cultured neurons (Li et al., 1993; Kim et al., 2012). In support of the notion of direct neuroprotection by FP receptor antagonism, AL-8810 proved to sustain the viability of cultured neurons exposed to oxygen-glucose deprivation (OGD), reduced the production of reactive oxygen species in OGD-stressed hippocampal slices, and suppressed the OGD-induced rise of intraneuronal Ca^{2+} concentration (Kim et al., 2012). It is noteworthy that intracellular Ca^{2+}

concentration increases considerably with SD itself, and may prove deleterious to neurons (Dietz et al., 2009). The Ca^{2+} overload with SD was previously prevented by the NMDA receptor antagonist ketamine (Reinhart and Shuttleworth, 2018). In addition, the L-type voltage-gated Ca^{2+} channel blocker nimodipine shortened SD duration similar to that achieved with ketamin (Szabó, 2019; Tóth, 2020). Therefore, it may well be, that a potential reduction of intracellular Ca^{2+} content by AL-8810 – as shown in neuronal cell culture (Kim et al., 2012) – could have contributed directly to shortened SD duration (Fig. 3), and the limitation of SD-related apoptosis (Fig. 5) as seen here.

The impact of AL-8810 treatment on microglia was evaluated here, as well, because microglia were found to be richly endowed with FP receptors (Fig. 6C). Previously, cultured rat microglia were shown not to express FP receptor mRNA (Kitanaka et al., 1996), yet, later investigation identified functional FP receptors on transformed human brain microglial cells (Xu et al., 2009). Further, in a model of experimental TBI, AL-8810 administration attenuated microglia proliferation days after the primary impact (Glushakov et al., 2013). In our experiments, microglia activation proved to be enhanced in the cortex ipsilateral to SD recurrence and the open cranial window, in addition to that caused by ischemia alone. Our previous data have shown that the surgical procedure itself (i.e. craniotomy) causes microglia activation, and recurrent SDs enhance it further (Tóth, 2020), which amounts to the difference observed between the ipsi- and contralateral hemispheres in our preparations (Fig. 5D-E). AL-8810 did not alter microglia activation at this time point after the primary insult (i.e. 5 h after ischemia onset, and 3 h after the occurrence of recurrent SDs). This suggests that even though microglia abundantly express FP receptors (Fig. 6C), these may not be functionally linked to microglia activation by endogenous PGF2α in the acute/subacute phase of cerebral ischemia.

Recurrent SDs propagating over cerebrocortical zones under metabolic stress have been increasingly more appreciated as the electrophysiological correlate of and pathophysiological contributor to ischemic injury progression (Dreier, 2011; Hartings et al., 2017a,b). Options for the pharmacological restriction of SD occurrence in acute brain injury patients have been, therefore, explored and debated intensively (Carlson et al., 2018, 2019; Sugimoto et al., 2018; Helbok et al., 2019). The clinical evidence gathered so far supports the inhibition of SD with the non-selective NMDA receptor antagonist and sedative agent ketamine (Hertle et al., 2012; Carlson et al., 2018), and experimental research has identified the L-type voltage-gated Ca^{2+} channel blocker nimodipine, as an additional, promising candidate for SD restriction (Dreier et al., 2002; Carlson et al., 2019; Szabó, 2019; Tóth, 2020). Our current experiments together with our previous results (Varga et al., 2016) suggest that prostaglandin signaling may be considered as an alternative or complementary target for intervention with therapeutic potential.

Data statement

The raw datasets generated and analyzed for this study can be viewed on request from the Authors.

Funding

00006 to EF, GINOP-2.3.2-15-2016-00020 and GINOP-2.3.2-15-2016-0034 to IAK), and the EU-funded Hungarian grant No. EFOP-3.6.1-16-2016-00008 to EF.

Declaration of Competing Interest

None.

References

Andreasson, K., 2010 Apr. Emerging roles of PGE2 receptors in models of neurological disease. Prostagland. Other Lipid Mediat. 91 (3–4), 104–112.

Astin, M., Stjernschantz, J., 1997 Dec 11. Mechanism of prostaglandin E2-, F2alpha- and latanoprost acid-induced relaxation of submental veins. Eur. J. Pharmacol. 340 (2–3), 195–201.

Ayata, C., Lauritzen, M., 2015 Jul. Spreading depression, spreading depolarizations, and the cerebral vasculature. Physiol. Rev. 95 (3), 953–993.

Bere, Z., Obrenovitch, T.P., Kozák, G., Bari, F., Farkas, E., 2014 Oct. Imaging reveals the focal area of spreading depolarizations and a variety of hemodynamic responses in a rat microembolic stroke model. J. Cereb. Blood Flow Metab. 34 (10), 1695–1705.

Candelario-Jalil, E., Fiebich, B.L., 2008. Cyclooxygenase inhibition in ischemic brain injury. Curr. Pharm. Des. 14 (14), 1401–1418.

Carlson, A.P., Abbas, M., Alunday, R.L., Qeadan, F., Shuttleworth, C.W., 2018 May 25. Spreading depolarization in acute brain injury inhibited by ketamine: a prospective, randomized, multiple crossover trial. J. Neurosurg. 1–7.

Carlson, A.P., Hänggi, D., Macdonald, R.L., Shuttleworth, C.W., 2019 Sep 27. Nimodipine reappraised: an old drug with a future. Curr. Neuropharmacol. https://doi.org/10.2174/1570159X17666190927113021. (Epub ahead of print).

Chen, J., Champa-Rodriguez, M.L., Woodward, D.F., 1995 Dec. Identification of a prostanoid FP receptor population producing endothelium-dependent vasorelaxation in the rabbit jugular vein. Br. J. Pharmacol. 116 (7), 3035–3041.

Claassen, J., Hirsch, L.J., Kreiter, K.T., Du, E.Y., Connolly, E.S., Emerson, R.G., Mayer, S.A., 2004 Dec. Quantitative continuous EEG for detecting delayed cerebral ischemia in patients with poor-grade subarachnoid hemorrhage. Clin. Neurophysiol. 115 (12), 2699–2710.

Davoli, M.A., Fourtounis, J., Tam, J., Xanthoudakis, S., Nicholson, D., Robertson, G.S., Ng, G.Y., Xu, D., 2002. Immunohistochemical and biochemical assessment of caspase-3 activation and DNA fragmentation following transient focal ischemia in the rat. Neuroscience. 115 (1), 125–136.

Dietz, R.M., Weiss, J.H., Shuttleworth, C.W., 2009 May. Contributions of Ca2+ and Zn2+ to spreading depression-like events and neuronal injury. J. Neurochem. 109 (Suppl. 1), 145–152.

Dreier, J.P., 2011 Apr. The role of spreading depression, spreading depolarization and spreading ischemia in neurological disease. Nat. Med. 17 (4), 439–447.

Dreier, J.P., Körner, K., Ebert, N., Görner, A., Rubin, I., Back, T., Lindauer, U., Wolf, T., Villringer, A., Einhäupl, K.M., Lauritzen, M., Dirnagl, U., 1998 Sep. Nitric oxide scavenging by hemoglobin or nitric oxide synthase inhibition by N-nitro-L-arginine induces cortical spreading ischemia when K+ is increased in the subarachnoid space. J. Cereb. Blood Flow Metab. 18 (9), 978–990.

Dreier, J.P., Windmüller, O., Petzold, G., Lindauer, U., Einhäupl, K.M., Dirnagl, U., 2002 Dec. Ischemia triggered by red blood cell products in the subarachnoid space is inhibited by nimodipine administration or moderate volume expansion/hemodilution in rats. Neurosurgery. 51 (6), 1457–1465 (discussion 1465-7).

Dreier, J.P., Woitzik, J., Fabricius, M., Bhatia, R., Major, S., Drenckhahn, C., Lehmann, T.N., Sarrafzadeh, A., Willumsen, L., Hartings, J.A., Sakowitz, O.W., Seemann, J.H., Thieme, A., Lauritzen, M., Strong, A.J., 2006 Dec. Delayed ischaemic neurological deficits after subarachnoid haemorrhage are associated with clusters of spreading depolarizations. Brain. 129 (Pt 12), 3224–3237.

Dreier, J.P., Major, S., Manning, A., Woitzik, J., Drenckhahn, C., Steinbrink, J., Tolias, C., Oliveira-Ferreira, A.I., Fabricius, M., Hartings, J.A., Vajkoczy, P., Lauritzen, M., Dirnagl, U., Bohner, G., Strong, A.J., COSBID Study Group, 2009 Jul. Cortical spreading ischaemia is a novel process involved in ischaemic damage in patients with aneurysmal subarachnoid haemorrhage. Brain. 132 (Pt 7), 1866–1881.

Eriksen, N., Rostrup, E., Fabricius, M., Scheel, M., Major, S., Winkler, M.K.L., Bohner, G., Santos, E., Sakowitz, O.W., Kola, V., Reiffurth, C., Hartings, J.A., Vajkoczy, P., Woitzik, J., Martus, P., Lauritzen, M., Pakkenberg, B., Dreier, J.P., 2019 Jan 22. Early focal brain injury after subarachnoid hemorrhage correlates with spreading depolarizations. Neurology. 92 (4), e326–e341.

Farkas, E., Obrenovitch, T.P., Institóris, Á., Bari, F., 2011 Sep. Effects of early aging and cerebral hypoperfusion on spreading depression in rats. Neurobiol. Aging 32 (9), 1707–1715.

Fricker, M., Tolkovsky, A.M., Borutaite, V., Coleman, M., Brown, G.C., 2018 Apr 1. Neuronal cell death. Physiol. Rev. 98 (2), 813–880.

Gariepy, H., Zhao, J., Levy, D., 2017 Mar. Differential contribution of COX-1 and COX-2 derived prostanoids to cortical spreading depression-evoked cerebral oligemia. J. Cereb. Blood Flow Metab. 37 (3), 1060–1068.

Gaudet, R.J., Levine, L., 1980 Nov-Dec. Effect of unilateral common carotid artery occlusion on levels of prostaglandins D2, F2 alpha and 6-keto-prostaglandin F1 alpha in gerbil brain. Stroke. 11 (6), 648–652.

Glushakov, A.V., Robbins, S.W., Bracy, C.L., Narumiya, S., Doré, S., 2013 Oct 30. Prostaglandin F2α FP receptor antagonist improves outcomes after experimental traumatic brain injury. J. Neuroinflammation 10, 132.

Hartings, J.A., Bullock, M.R., Okonkwo, D.O., Murray, L.S., Murray, G.D., Fabricius, M., Maas, A.I., Woitzik, J., Sakowitz, O., Mathern, B., Roozenbeek, B., Lingsma, H., Dreier, J.P., Puccio, A.M., Shutter, L.A., Pahl, C., Strong, A.J., 2011 Deca. Co-operative study on brain injury depolarisations. Spreading depolarisations and outcome after traumatic brain injury: a prospective observational study. Lancet Neurol. 10 (12), 1058–1064.

Hartings, J.A., Watanabe, T., Bullock, M.R., Okonkwo, D.O., Fabricius, M., Woitzik, J., Dreier, J.P., Puccio, A., Shutter, L.A., Pahl, C., Strong, A.J., 2011 Mayb. Co-operative study on brain injury depolarizations. Spreading depolarizations have prolonged direct current shifts and are associated with poor outcome in brain trauma. Brain. 134 (Pt 5), 1529–1540.

Hartings, J.A., Shuttleworth, C.W., Kirov, S.A., Ayata, C., Hinzman, J.M., Foreman, B., Andrew, R.D., Boutelle, M.G., Brennan, K.C., Carlson, A.P., Dahlem, M.A., Drenckhahn, C., Dohmen, C., Fabricius, M., Farkas, E., Feuerstein, D., Graf, R., Helbok, R., Lauritzen, M., Major, S., Oliveira-Ferreira, A.I., Richter, F., Rosenthal, E.S., Sakowitz, O.W., Sánchez-Porras, R., Santos, E., Schöll, M., Strong, A.J., Urbach, A., Westover, M.B., Winkler, M.K., Witte, O.W., Woitzik, J., Dreier, J.P., 2017 Mya. The continuum of spreading depolarizations in acute cortical lesion development: examining Leão's legacy. J. Cereb. Blood Flow Metab. 37 (5), 1571–1594.

Hartings, J.A., York, J., Carroll, C.P., Hinzman, J.M., Mahoney, E., Krueger, B., Winkler, M.K.L., Major, S., Horst, V., Jahnke, P., Woitzik, J., Kola, V., Du, Y., Hagen, M., Jiang, J., Dreier, J.P., 2017 1b. Subarachnoid blood acutely induces spreading depolarizations and early cortical infarction. Brain. 140 (10), 2673–2690.

Hayashi, S., Park, M.K., Kuehl, T.J., 1985 Jun. Relaxant and contractile responses to prostaglandins in premature, newborn and adult baboon cerebral arteries. J. Pharmacol. Exp. Ther. 233 (3), 628–635.

Helbok, R., Hartings, J.A., Schiefecker, A., Balança, B., Jewel, S., Foreman, B., Ercole, A., Balu, R., Ayata, C., Ngwenya, L., Rosenthal, E., Boutelle, M.G., Farkas, E., Dreier, J.P., Fabricius, M., Shuttleworth, C.W., Carlson, A., 2019 Jul 23. What should a clinician do when spreading depolarizations are observed in a patient? Neurocrit. Care. https://doi.org/10.1007/s12028-019-00777-6. (Epub ahead of print).

Hertelendy, P., Varga, D.P., Menyhárt, Á., Bari, F., Farkas, E., 2019 Jul. Susceptibility of the cerebral cortex to spreading depolarization in neurological disease states: the impact of aging. Neurochem. Int. 127, 125–136.

Hertle, D.N., Dreier, J.P., Woitzik, J., Hartings, J.A., Bullock, R., Okonkwo, D.O., Shutter, L.A., Vidgeon, S., Strong, A.J., Kowoll, C., Dohmen, C., Diedler, J., Veltkamp, R., Bruckner, T., Unterberg, A.W., Sakowitz, O.W., Cooperative Study of Brain Injury Depolarizations (COSBID), 2012 Aug. Effect of analgesics and sedatives on the occurrence of spreading depolarizations accompanying acute brain injury. Brain. 135 (Pt 8), 2390–2398.

Katz, B., Sofonio, M., Lyden, P.D., Mitchell, M.D., 1988 Mar. Prostaglandin concentrations in cerebrospinal fluid of rabbits under normal and ischemic conditions. Stroke. 19 (3), 349–351.

Kim, Y.T., Moon, S.K., Maruyama, T., Narumiya, S., Doré, S., 2012 Oct. Prostaglandin FP receptor inhibitor reduces ischemic brain damage and neurotoxicity. Neurobiol. Dis. 48 (1), 58–65.

Kitanaka, J., Hasimoto, H., Sugimoto, Y., Negishi, M., Aino, H., Gotoh, M., Ichikawa, A., Baba, A., 1994 Jul. Cloning and expression of a cDNA for rat prostaglandin F2 alpha receptor. Prostaglandins. 48 (1), 31–41.

Kitanaka, J., Hashimoto, H., Gotoh, M., Kondo, K., Sakata, K., Hirasawa, Y., Sawada, M., Suzumura, A., Marunouchi, T., Matsuda, T., Baba, A., 1996 Jan 29. Expression pattern of messenger RNAs for prostanoid receptors in glial cell cultures. Brain Res. 707 (2), 282–287.

Lauritzen, M., Hansen, A.J., Kronborg, D., Wieloch, T., 1990 Jan. Cortical spreading depression is associated with arachidonic acid accumulation and preservation of energy charge. J. Cereb. Blood Flow Metab. 10 (1), 115–122.

Leão, A.A.P., 1944. Spreading depression of activity in the cerebral cortex. J. Neurophysiol. 7, 359–390.

Li, D.Y., Varma, D.R., Chatterjee, T.K., Fernandez, H., Abran, D., Chemtob, S., 1993 Dec. Fewer PGE2 and PGF2 alpha receptors in brain synaptosomes of newborn than of adult pigs. J. Pharmacol. Exp. Ther. 267 (3), 1292–1297.

Li, D.Y., Varma, D.R., Chemtob, S., 1994 May. Ontogenic increase in PGE2 and PGF2 alpha receptor density in brain microvessels of pigs. Br. J. Pharmacol. 112 (1), 59–64.

Lückl, J., Lemale, C.L., Kola, V., Horst, V., Khojasteh, U., Oliveira-Ferreira, A.I., Major, S., Winkler, M.K.L., Kang, E.J., Schoknecht, K., Martus, P., Hartings, J.A., Woitzik, J., Dreier, J.P., 2018 Jun 1. The negative ultraslow potential, electrophysiological correlate of infarction in the human cortex. Brain. 141 (6), 1734–1752.

Manabat, C., Han, B.H., Wendland, M., Derugin, N., Fox, C.K., Choi, J., Holtzman, D.M., Ferriero, D.M., Vexler, Z.S., 2003 Jan. Reperfusion differentially induces caspase-3 activation in ischemic core and penumbra after stroke in immature brain. Stroke. 34 (1), 207–213.

Menyhárt, Á., Makra, P., Szepes, B., Tóth, O.M., Hertelendy, P., Bari, F., Farkas, E., 2015 Dec. High incidence of adverse cerebral blood flow responses to spreading depolarization in the aged ischemic rat brain. Neurobiol. Aging 36 (12), 3269–3277.

Menyhárt, Á., Farkas, A.E., Varga, D.P., Frank, R., Tóth, R., Bálint, A.R., Makra, P., Dreier, J.P., Bari, F., Krizbai, I.A., Farkas, E., 2018 Nov. Large-conductance Ca2+ −activated potassium channels are potently involved in the inverse neurovascular response to spreading depolarization. Neurobiol. Dis. 119, 41–52.

Ogawa, H., Sasaki, T., Kassell, N.F., Nakagomi, T., Lehman, R.M., Hongo, K., 1987. Immunohistochemical demonstration of increase in prostaglandin F2-alpha after recirculation in global ischemic rat brains. Acta Neuropathol. 75 (1), 62–68.

Pinczolits, A., Zdunczyk, A., Dengler, N.F., Hecht, N., Kowoll, C.M., Dohmen, C., Graf, R., Winkler, M.K., Major, S., Hartings, J.A., Dreier, J.P., Vajkoczy, P., Woitzik, J., 2017 May. Standard-sampling microdialysis and spreading depolarizations in patients with malignant hemispheric stroke. J. Cereb. Blood Flow Metab. 37 (5), 1896–1905.

Reinhart, K.M., Shuttleworth, C.W., 2018 Jul. Ketamine reduces deleterious consequences of spreading depolarizations. Exp. Neurol. 305, 121–128.

Rice, K.M., Uddemarri, S., Desai, D.H., Morrison, R.G., Harris, R., Wright, G.L., Blough, E.R., 2008 Feb. PGF2alpha-associated vascular smooth muscle hypertrophy is ROS dependent and involves the activation of mTOR, p70S6k, and PTEN. Prostagland. Other Lipid Mediat. 85 (1–2), 49–57.

Rots, M.L., van Putten, M.J., Hoedemaekers, C.W., Horn, J., 2016 Apr. Continuous EEG monitoring for early detection of delayed cerebral ischemia in subarachnoid hemorrhage: a pilot study. Neurocrit. Care. 24 (2), 207–216.

Saleem, S., Ahmad, A.S., Maruyama, T., Narumiya, S., Doré, S., 2009 Jan. PGF(2alpha) FP receptor contributes to brain damage following transient focal brain ischemia. Neurotox. Res. 15 (1), 62–70.

Sánchez-Porras, R., Santos, E., Schöll, M., Kunzmann, K., Stock, C., Silos, H., Unterberg, A.W., Sakowitz, O.W., 2017 May. Ketamine modulation of the haemodynamic response to spreading depolarization in the gyrencephalic swine brain. J. Cereb. Blood Flow Metab. 37 (5), 1720–1734.

Santilli, F., Boccatonda, A., Davì, G., Cipollone, F., 2016 Jun. The Coxib case: are EP receptors really guilty? Atherosclerosis. 249, 164–173.

Schmidt, M., Hováth-Puhó, E., Christiansen, C.F., Petersen, K.L., Bøtker, H.E., Sørensen, H.T., 2014 Nov 25. Preadmission use of nonaspirin nonsteroidal anti-inflammatory drugs and 30-day stroke mortality. Neurology. 83 (22), 2013–2022.

Sharif, N.A., Klimko, P.G., 2019 Apr. Prostaglandin FP receptor antagonists: discovery, pharmacological characterization and therapeutic utility. Br. J. Pharmacol. 176 (8), 1059–1078.

Shibata, M., Leffler, C.W., Busija, D.W., 1992 Feb 14. Pial arteriolar constriction following cortical spreading depression is mediated by prostanoids. Brain Res. 572 (1–2), 190–197.

Shuttleworth, C.W., Andrew, R.D., Akbari, Y., Ayata, C., Balu, R., Brennan, K.C., Boutelle, M., Carlson, A.P., Dreier, J.P., Fabricius, M., Farkas, E., Foreman, B., Helbok, R., Henninger, N., Jewell, S.L., Jones, S.C., Kirov, S.A., Lindquist, B.E., Maciel, C.B., Okonkwo, D., Reinhart, K.M., Robertson, R.M., Rosenthal, E.S., Watanabe, T., Hartings, J.A., 2019 Aug 6. Which spreading depolarizations are deleterious to brain tissue? Neurocrit. Care. https://doi.org/10.1007/s12028-019-00776-7. (Epub ahead of print).

Somjen, G.G., 2001 Jul. Mechanisms of spreading depression and hypoxic spreading depression-like depolarization. Physiol. Rev. 81 (3), 1065–1096.

Sugimoto, K., Nomura, S., Shirao, S., Inoue, T., Ishihara, H., Kawano, R., Kawano, A., Oka, F., Suehiro, E., Sadahiro, H., Shinoyama, M., Oku, T., Maruta, Y., Hirayama, Y., Hiyoshi, K., Kiyohira, M., Yoneda, H., Okazaki, K., Dreier, J.P., Suzuki, M., 2018 Dec. Cilostazol decreases duration of spreading depolarization and spreading ischemia after aneurysmal subarachnoid hemorrhage. Ann. Neurol. 84 (6), 873–885.

Szabó, Í., M Tóth, O., Török, Z., Varga, D.P., Menyhárt, Á., Frank, R., Hantosi, D., Hunya, Á., Bari, F., Horváth, I., Vigh, L., Farkas, E., 2019 May. The impact of dihydropyridine derivatives on the cerebral blood flow response to somatosensory stimulation and spreading depolarization. Br. J. Pharmacol. 176 (9), 1222–1234. https://doi.org/10.1111/bph.14611.

Tóth, O.M., Menyhárt, Á., Varga, V.É., Hantosi, D., Ivánkovits-Kiss, O., Varga, D.P., Szabó, Í., Janovák, L., Dékány, I., Farkas, E., Bari, F., 2020 Jan 1. Chitosan nanoparticles release nimodipine in response to tissue acidosis to attenuate spreading depolarization evoked during forebrain ischemia. Neuropharmacology. 162 (107850), 107850. https://doi.org/10.1016/j.neuropharm.2019.107850.

Toth, P., Szarka, N., Farkas, E., Ezer, E., Czeiter, E., Amrein, K., Ungvari, Z., Hartings, J.A., Buki, A., Koller, A., 2016 Nov 1. Traumatic brain injury-induced autoregulatory dysfunction and spreading depression-related neurovascular uncoupling: pathomechanisms, perspectives, and therapeutic implications. Am. J. Physiol. Heart Circ. Physiol. 311 (5), H1118–H1131.

Varga, D.P., Puskás, T., Menyhárt, Á., Hertelendy, P., Zölei-Szénási, D., Tóth, R., Ivánkovits-Kiss, O., Bari, F., Farkas, E., 2016 Aug 10. Contribution of prostanoid signaling to the evolution of spreading depolarization and the associated cerebral blood flow response. Sci. Rep. 6, 31402.

Woitzik, J., Hecht, N., Pinczolits, A., Sandow, N., Major, S., Winkler, M.K., Weber-Carstens, S., Dohmen, C., Graf, R., Strong, A.J., Dreier, J.P., Vajkoczy, P., COSBID Study Group, 2013 Mar 19. Propagation of cortical spreading depolarization in the human cortex after malignant stroke. Neurology. 80 (12), 1095–1102.

Xu, W., Chou, C.L., Israel, D.D., Hutchinson, A.J., Regan, J.W., 2009 Apr 17. PGF(2alpha) stimulates FP prostanoid receptor mediated crosstalk between Ras/Raf signaling and Tcf transcriptional activation. Biochem. Biophys. Res. Commun. 381 (4), 625–629.

Yu, Y., Lucitt, M.B., Stubbe, J., Cheng, Y., Friis, U.G., Hansen, P.B., Jensen, B.L., Smyth, E.M., FitzGerald, G.A., 2009 May 12. Prostaglandin F2alpha elevates blood pressure and promotes atherosclerosis. Proc. Natl. Acad. Sci. U. S. A. 106 (19), 7985–7990.

Yu, Z., Wen, D., Zheng, J., Guo, R., Li, H., C1, Y., Ma, L., 2019 Jun. Predictive accuracy of alpha-delta ratio on quantitative electroencephalography for delayed cerebral ischemia in patients with aneurysmal subarachnoid hemorrhage: meta-analysis. World Neurosurg. 126, e510–e516.

Zannoni, A., Bernardini, C., Rada, T., Ribeiro, L.A., Forni, M., Bacci, M.L., 2007 Jul 20. Prostaglandin F2-alpha receptor (FPr) expression on porcine corpus luteum microvascular endothelial cells (pCL-MVECs). Reprod. Biol. Endocrinol. 5, 31.

Zhang, J., Gong, Y., Yu, Y., 2010 Oct 14. PG F(2α) receptor: a promising therapeutic target for cardiovascular disease. Front. Pharmacol. 1, 116.